Extension and generalization of the Gay-Berne potential

Douglas J. Cleaver,[1,2] Christopher M. Care,[1,2] Michael P. Allen,[3] and Maureen P. Neal[4]
[1]*Division of Applied Physics, Sheffield Hallam University, Pond Street, Sheffield S1 1WB, United Kingdom*
[2]*Materials Research Institute, Sheffield Hallam University, Pond Street, Sheffield S1 1WB, United Kingdom*
[3]*H.H. Wills Physics Laboratory, Tyndall Avenue, Bristol BS8 1TL, United Kingdom*
[4]*Department of Mathematics, University of Derby, Kedleston Road, Derby DE22 1GB, United Kingdom*
(Received 23 January 1995)

In this paper, we report a generalized form for the range parameter governing the pair interaction between soft ellipsoidal particles. For nonequivalent uniaxial particles, we extend the Berne-Pechukas Gaussian overlap formalism to obtain an explicit expression for this range parameter. We confirm that this result is identical to that given by an approach that is not widely recognized, based on an approximation to the Perram-Wertheim hard-ellipsoid contact function. We further illustrate the power of the latter route by using it to write down the range parameter for the interaction between two nonequivalent *biaxial* particles. An explicit interaction potential for nonequivalent uniaxial particles is obtained by importing the uniaxial range parameter result into the standard Gay-Berne form. A parametrization of this potential is investigated for a rod-disk interaction. [S1063-651X(96)05506-7]

PACS number(s): 61.30.Cz, 34.20.Gj, 07.05.Tp, 61.20.Ja

I. INTRODUCTION

Following the original work performed using models with purely steric interactions [1–3], there has been a growing interest in computer simulations of liquid-crystalline systems using models with ''soft'' potentials [3]. For computational efficiency, most of the models used in the latter have employed a single anisotropic interaction site per molecule; in some cases, a purely attractive anisotropic term has been combined with a spherical core to produce mesogenic behavior [4,5]. While there have been some simulations performed with idealized [6] and realistic [7] models based on a multisite Lennard-Jones approach, the various single-site anisotropic forms available continue to offer a productive route by which to study order in liquids.

The standard among these anisotropic pair interactions is the Gay-Berne potential [8]. This uses an approximately ellipsoidal range parameter [9] in a shifted Lennard-Jones form combined with a similarly anisotropic well-depth function. This range parameter was originally derived by Berne and Pechukas on the basis of the overlap of two ellipsoidal Gaussian distributions [9]. Various parametrizations of this model have been used to study the phase behavior of calamitic liquid crystals: nematic and smectic phases have been observed by several groups [10]. A discotic parametrization has also been studied and shown to give nematic discotic and columnar phases [11]. Very recently, Berardi, Fava, and Zannoni have reported a biaxial version of the Gay-Berne potential [12].

The development of large parallel machines, possessing computational power equivalent to some hundreds of workstations, offers the possibility of far more ambitious simulations, using tens of thousands of interaction sites rather than the few thousand currently used in typical Gay-Berne simulations. This increase can be exploited either by enhancing the complexity of the model potentials used (e.g., moving to atomistic representations) or by enlarging the system size and continuing to work with idealized potentials.

In seeking a realistically attainable route by which to model some of the more exotic (and technologically useful) liquid crystalline phases, a compromise between these two positions seems a promising path: the cylindrically symmetric anisotropic potentials currently in use appear inadequate, while (computationally expensive) atomistic models do not represent an efficient means by which to study phase behavior. Models comprising several anisotropic sites per molecule therefore appear to offer a reasonable option (indeed, this was the basis of the original Berne and Pechukas paper [9] from which the Gay-Berne potential evolved).

This option is already available to some extent in that assemblies of identical Gay-Berne units and Lennard-Jones sites can be simulated using the potentials currently available; initial studies of such assemblies have already been attempted [13,14]. The restriction to identical Gay-Berne units is clearly a disadvantage, however, when one considers the range of structures adopted by real molecules.

In this paper we propose a generalization of the Gay-Berne potential, which yields the interaction between nonequivalent uniaxial particles (e.g., one oblate and one prolate). This is achieved by extending the range parameter function, on which the shape of the Gay-Berne potential is based, to incorporate mixed interactions. We confirm that, as pointed out by Perram *et al.* [15] and echoed in [2], this function can also be obtained from an approximation to the Perram-Wertheim hard-ellipsoid contact function [16]. Since the Perram-Wertheim expression for the hard-ellipsoid contact function holds for nonequivalent biaxial particles, we are able to invoke this same approximation to obtain the form of the Gaussian overlap range parameter for this general case.

The equivalence of the Gaussian overlap and the approximate hard-ellipsoid contact function routes to the range parameter is not widely recognized. To emphasize this equivalence, both are presented in Sec. III. We stress that the resulting expressions are obtainable from existing results [see, e.g., Eqs. (2.85)–(2.96) of [2]], but consider the Gaussian overlap approach to be worthwhile since it provides the

range parameter with its physical significance. We also note that the simple forms of our final expressions lend them considerable practical utility.

The main motivation for the work presented in this paper is the extension of the range of anisotropic multisite models, although its application to mixtures of different single-site particles is also clear. Thus, this extended version of the potential is expected to be of use in studying a range of physical systems for which the original Gay-Berne potential is inappropriate.

The remainder of the paper is arranged as follows. In the next section, we describe Berne and Pechuka's formulation of the overlap problem for identical particles, and its application in the Gay-Berne potential. Section III contains the range parameter derivations described above. Using the uniaxial particle result as a basis, we then develop an extension of the Gay-Berne potential for two nonequivalent particles. Finally, this potential is examined for the case of a disk interacting with a rod, and a parametrization is calculated and discussed.

II. THE ORIGINAL MODEL (IDENTICAL UNIAXIAL PARTICLES)

In their original treatment of the interaction between two elongated molecules, Berne and Pechukas [9] considered the case where each molecule is approximated by a uniaxially stretched Gaussian distribution of the form

$$G(\mathbf{r}) = |\underline{\gamma}|^{-1/2} \exp[-\mathbf{r}\cdot\underline{\gamma}^{-1}\cdot\mathbf{r}]$$

where $\underline{\gamma}$ is the matrix

$$\underline{\gamma} = (l^2-d^2)\underline{\hat{\mathbf{u}}\hat{\mathbf{u}}} + d^2\underline{\mathbf{I}} \tag{1}$$

and l and d scale the length and breadth, respectively. $\underline{\mathbf{I}}$ is the identity matrix and $\hat{\mathbf{u}}$ is a unit vector along the principal axis of the particle. Surfaces of constant $G(\mathbf{r})$ are ellipsoids of revolution about this axis. By taking the interaction to be dependent on the overlap of two similarly stretched Gaussian distributions, Berne and Pechukas expressed the pair potential in terms of the orientation-dependent range parameter

$$\sigma^2(\hat{\mathbf{u}}_i,\hat{\mathbf{u}}_j,\hat{\mathbf{r}}_{ij}) = \frac{r_{ij}^2}{\mathbf{r}_{ij}\cdot(\underline{\gamma_i+\gamma_j})^{-1}\cdot\mathbf{r}_{ij}}, \tag{2}$$

where $\mathbf{r}_{ij} = r_{ij}\hat{\mathbf{r}}_{ij}$ is the vector linking the centers of mass of the two particles i and j. When the two particles are identical, the eigenvectors of $\underline{\gamma_i+\gamma_j}$ are $\hat{\mathbf{u}}_i \pm \hat{\mathbf{u}}_j$ and their cross product. Equation (2) then reduces to [8]

$$\sigma(\hat{\mathbf{u}}_i,\hat{\mathbf{u}}_j,\hat{\mathbf{r}}_{ij}) = \sigma_0\left[1-\frac{\chi}{2}\left\{\frac{(\hat{\mathbf{r}}_{ij}\cdot\hat{\mathbf{u}}_i+\hat{\mathbf{r}}_{ij}\cdot\hat{\mathbf{u}}_j)^2}{1+\chi\hat{\mathbf{u}}_i\cdot\hat{\mathbf{u}}_j} + \frac{(\hat{\mathbf{r}}_{ij}\cdot\hat{\mathbf{u}}_i-\hat{\mathbf{r}}_{ij}\cdot\hat{\mathbf{u}}_j)^2}{1-\chi\hat{\mathbf{u}}_i\cdot\hat{\mathbf{u}}_j}\right\}\right]^{-1/2}, \tag{3}$$

where $\sigma_0 = \sqrt{2}d$ and

$$\chi = [(l/d)^2-1]/[(l/d)^2+1]. \tag{4}$$

In their formulation of the problem, Berne and Pechukas used their range parameter in a potential of the stretched Gaussian form

$$U(\hat{\mathbf{u}}_i,\hat{\mathbf{u}}_j,\mathbf{r}_{ij}) = \varepsilon_0\varepsilon_1(\hat{\mathbf{u}}_i,\hat{\mathbf{u}}_j)\exp[-r_{ij}^2/\sigma^2(\hat{\mathbf{u}}_i,\hat{\mathbf{u}}_j,\hat{\mathbf{r}}_{ij})], \tag{5}$$

where ε_0 is the well-depth parameter and the strength anisotropy function is given by

$$\varepsilon_1(\hat{\mathbf{u}}_i,\hat{\mathbf{u}}_j) = [1-\chi^2(\hat{\mathbf{u}}_i\cdot\hat{\mathbf{u}}_j)^2]^{-1/2}. \tag{6}$$

In the ensuing years, several extensions and refinements were made to this basic potential (see [17] for a brief review) in order to remove some of its more unrealistic features. The most notable of these were the replacement of the stretched Gaussian potential of (5) with a Lennard-Jones form [18] and, subsequently, a shifted Lennard-Jones form [8]. Thus, in the contemporary Gay-Berne model, the interaction is written as

$$U(\hat{\mathbf{u}}_i,\hat{\mathbf{u}}_j,\mathbf{r}_{ij}) = 4\varepsilon(\hat{\mathbf{u}}_i,\hat{\mathbf{u}}_j,\hat{\mathbf{r}}_{ij})\left[\left(\frac{\sigma_0}{r_{ij}-\sigma(\hat{\mathbf{u}}_i,\hat{\mathbf{u}}_j,\hat{\mathbf{r}}_{ij})+\sigma_0}\right)^{12} - \left(\frac{\sigma_0}{r_{ij}-\sigma(\hat{\mathbf{u}}_i,\hat{\mathbf{u}}_j,\hat{\mathbf{r}}_{ij})+\sigma_0}\right)^{6}\right], \tag{7}$$

where the strength anisotropy function is now

$$\varepsilon(\hat{\mathbf{u}}_i,\hat{\mathbf{u}}_j,\hat{\mathbf{r}}_{ij}) = \varepsilon_0\varepsilon_1^{\nu}(\hat{\mathbf{u}}_i,\hat{\mathbf{u}}_j)\varepsilon_2^{\mu}(\hat{\mathbf{u}}_i,\hat{\mathbf{u}}_j,\hat{\mathbf{r}}_{ij}). \tag{8}$$

Here, the powers μ and ν are adjustable exponents and $\varepsilon_2(\hat{\mathbf{u}}_i,\hat{\mathbf{u}}_j,\hat{\mathbf{r}}_{ij})$ is given by

$$\varepsilon_2(\hat{\mathbf{u}}_i,\hat{\mathbf{u}}_j,\hat{\mathbf{r}}_{ij}) = 1-\frac{\chi'}{2}\left\{\frac{(\hat{\mathbf{r}}_{ij}\cdot\hat{\mathbf{u}}_i+\hat{\mathbf{r}}_{ij}\cdot\hat{\mathbf{u}}_j)^2}{1+\chi'\hat{\mathbf{u}}_i\cdot\hat{\mathbf{u}}_j} + \frac{(\hat{\mathbf{r}}_{ij}\cdot\hat{\mathbf{u}}_i-\hat{\mathbf{r}}_{ij}\cdot\hat{\mathbf{u}}_j)^2}{1-\chi'\hat{\mathbf{u}}_i\cdot\hat{\mathbf{u}}_j}\right\}. \tag{9}$$

The additional parameter, χ', is given by the ratio of end-end to side-side well depths via

$$\chi' = [1-(\varepsilon_E/\varepsilon_S)^{1/\mu}]/[1+(\varepsilon_E/\varepsilon_S)^{1/\mu}]. \tag{10}$$

While the form of the potential used to describe the interaction has been modified considerably since the original formulation, it is striking that the range parameter on which it is based, $\sigma(\hat{\mathbf{u}}_i,\hat{\mathbf{u}}_j,\hat{\mathbf{r}}_{ij})$, has remained unchanged from that obtained by Berne and Pechukas. In seeking a form for the interaction between *nonequivalent* ellipsoidal particles, we note that the range parameter of Eq. (3) lacks the required symmetries. What is required is a generalized equation for this fundamental quantity. In principle, this can then be inserted into any of the various forms of the potential function, though we shall concentrate on the Gay-Berne form.

III. GENERALIZATION OF THE RANGE PARAMETER FOR NONEQUIVALENT PARTICLES

A. Uniaxial ellipsoids via the Berne-Pechukas route

In the following, we consider two cylindrically symmetric, ellipsoidal particles, i and j, with lengths (breadths)

TABLE I. The relative positions and orientations of the five arrangements used to define the parameters of the well-depth anisotropy function. The figures illustrate the arrangements for a rodlike particle (molecule j) and a disklike particle (molecule i). These are differentiated by the marking of symmetry axes.

Configuration	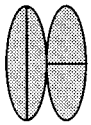	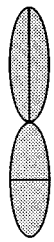	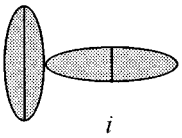	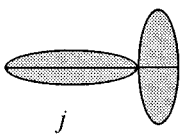	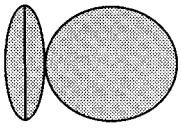
Label	T1	T2	S	E	X
$\hat{\mathbf{u}}_i \cdot \hat{\mathbf{u}}_j$	0	0	1	1	0
$\hat{\mathbf{u}}_i \cdot \hat{\mathbf{r}}_{ij}$	1	0	0	1	0
$\hat{\mathbf{u}}_j \cdot \hat{\mathbf{r}}_{ij}$	0	1	0	1	0
$\varepsilon(\hat{\mathbf{u}}_i, \hat{\mathbf{u}}_j, \hat{\mathbf{r}}_{ij})$	$\varepsilon_{T1} = \varepsilon_0[1-\chi'\alpha'^2]^{\mu}$	$\varepsilon_{T2} = \varepsilon_0[1-\chi'\alpha'^{-2}]^{\mu}$	$\varepsilon_S = \frac{\varepsilon_0}{(1-\chi^2)^{\nu/2}}$	$\varepsilon_E = \frac{\varepsilon_0}{(1-\chi^2)^{\nu/2}}\left[1-\chi'\left(\frac{\alpha'^2+\alpha'^{-2}-2\chi'}{1-\chi'^2}\right)\right]^{\mu}$	$\varepsilon_X = \varepsilon_0$

scaled by l_i and l_j (d_i and d_j), respectively. We place no restrictions on the values of the length and breadth variables, so that each of the particles can be oblate, prolate, or spherical. In Table I, we list and label the five independent arrangements for which the dot products of $\hat{\mathbf{u}}_i$, $\hat{\mathbf{u}}_j$, and $\hat{\mathbf{r}}_{ij}$ are all equal to either zero or unity.

Following Berne and Pechukas, we wish to define the range parameter, which governs the interaction, in terms of the overlap of two appropriately stretched Gaussians. To this end, we return to Eq. (2) and seek eigenvectors of the matrix

$$\underline{\gamma_i + \gamma_j} = \alpha_i \underline{\hat{\mathbf{u}}_i \hat{\mathbf{u}}_i} + \alpha_j \underline{\hat{\mathbf{u}}_j \hat{\mathbf{u}}_j} + \beta \underline{\mathbf{I}}, \tag{11}$$

where $\alpha_i = l_i^2 - d_i^2$ and $\beta = d_i^2 + d_j^2$. The orthonormal eigenvectors of this matrix are

$$\hat{\mathbf{e}}_1 = \frac{\alpha_i\sqrt{\alpha_j}(\hat{\mathbf{u}}_i \cdot \hat{\mathbf{u}}_j)y\hat{\mathbf{u}}_i + \sqrt{\alpha_j}\hat{\mathbf{u}}_j}{\{(\alpha_i + y^{-1})[1 + \alpha_i\alpha_j y^2(\hat{\mathbf{u}}_i \cdot \hat{\mathbf{u}}_j)^2]\}^{1/2}}, \tag{12a}$$

$$\hat{\mathbf{e}}_2 = \frac{\sqrt{\alpha_i}\hat{\mathbf{u}}_i - \alpha_j\sqrt{\alpha_i}(\hat{\mathbf{u}}_i \cdot \hat{\mathbf{u}}_j)y\hat{\mathbf{u}}_j}{\{(\alpha_j - y^{-1})[1 + \alpha_i\alpha_j y^2(\hat{\mathbf{u}}_i \cdot \hat{\mathbf{u}}_j)^2]\}^{1/2}} \tag{12b}$$

and their cross product. The corresponding eigenvalues are $\lambda_1 = \alpha_i + y^{-1} + \beta$, $\lambda_2 = \alpha_j - y^{-1} + \beta$, and $\lambda_3 = \beta$, where y satisfies the quadratic equation

$$y^2\alpha_i\alpha_j(\hat{\mathbf{u}}_i \cdot \hat{\mathbf{u}}_j)^2 + y(\alpha_j - \alpha_i) - 1 = 0. \tag{13}$$

In the case where the molecular axes are orthogonal, $\hat{\mathbf{e}}_1$ and $\hat{\mathbf{e}}_2$ reduce to $\hat{\mathbf{u}}_j$ and $\hat{\mathbf{u}}_i$, respectively. We also note that the eigenvectors and $(\hat{\mathbf{u}}_i \cdot \hat{\mathbf{u}}_j)y$ remain well behaved in the limit that α_i tends to α_j. Equations (11) to (13) can be combined to yield

$$\mathbf{r}_{ij} \cdot (\underline{\gamma_i + \gamma_j})^{-1} \cdot \mathbf{r}_{ij} = \frac{r_{ij}^2}{\beta}\left[1 - \frac{1}{[1 + \alpha_i\alpha_j y^2(\hat{\mathbf{u}}_i \cdot \hat{\mathbf{u}}_j)^2]}\left\{\frac{(\alpha_i\sqrt{\alpha_j}(\hat{\mathbf{u}}_i \cdot \hat{\mathbf{u}}_j)y\hat{\mathbf{u}}_i \cdot \hat{\mathbf{r}}_{ij} + \sqrt{\alpha_j}\hat{\mathbf{u}}_j \cdot \hat{\mathbf{r}}_{ij})^2}{\alpha_i + y^{-1} + \beta} + \frac{[\sqrt{\alpha_i}\hat{\mathbf{u}}_i \cdot \hat{\mathbf{r}}_{ij} - \alpha_j\sqrt{\alpha_i}(\hat{\mathbf{u}}_i \cdot \hat{\mathbf{u}}_j)y\hat{\mathbf{u}}_j \cdot \hat{\mathbf{r}}_{ij}]^2}{\alpha_j - y^{-1} + \beta}\right\}\right], \tag{14}$$

which can be inserted into Eq. (2) to give the generalized range parameter $\sigma(\hat{\mathbf{u}}_i, \hat{\mathbf{u}}_j, \hat{\mathbf{r}}_{ij})$. Further manipulation of Eq. (14) using (13) allows elimination of y to give

$$\sigma(\hat{\mathbf{u}}_i, \hat{\mathbf{u}}_j, \hat{\mathbf{r}}_{ij}) = \sigma_0\left[1 - \chi\left\{\frac{\alpha^2(\hat{\mathbf{r}}_{ij} \cdot \hat{\mathbf{u}}_i)^2 + \alpha^{-2}(\hat{\mathbf{r}}_{ij} \cdot \hat{\mathbf{u}}_j)^2 - 2\chi(\hat{\mathbf{r}}_{ij} \cdot \hat{\mathbf{u}}_i)(\hat{\mathbf{r}}_{ij} \cdot \hat{\mathbf{u}}_j)(\hat{\mathbf{u}}_i \cdot \hat{\mathbf{u}}_j)}{1 - \chi^2(\hat{\mathbf{u}}_i \cdot \hat{\mathbf{u}}_j)^2}\right\}\right]^{-1/2}, \tag{15}$$

where

$$\sigma_0 = \sqrt{d_i^2 + d_j^2}, \tag{16}$$

$$\chi = \left(\frac{(l_i^2 - d_i^2)(l_j^2 - d_j^2)}{(l_j^2 + d_i^2)(l_i^2 + d_j^2)} \right)^{1/2}, \tag{17}$$

and

$$\alpha^2 = \left(\frac{(l_i^2 - d_i^2)(l_j^2 + d_i^2)}{(l_j^2 - d_j^2)(l_i^2 + d_j^2)} \right)^{1/2}. \tag{18}$$

To make a closer comparison with the Berne-Pechukas form [i.e., Eq. (3)], we note that Eq. (15) can also be expressed as

$$\sigma(\hat{\mathbf{u}}_i, \hat{\mathbf{u}}_j, \hat{\mathbf{r}}_{ij}) = \sigma_0 \left[1 - \frac{\chi}{2} \left\{ \frac{(\alpha \hat{\mathbf{r}}_{ij} \cdot \hat{\mathbf{u}}_i + \alpha^{-1} \hat{\mathbf{r}}_{ij} \cdot \hat{\mathbf{u}}_j)^2}{1 + \chi \hat{\mathbf{u}}_i \cdot \hat{\mathbf{u}}_j} + \frac{(\alpha \hat{\mathbf{r}}_{ij} \cdot \hat{\mathbf{u}}_i - \alpha^{-1} \hat{\mathbf{r}}_{ij} \cdot \hat{\mathbf{u}}_j)^2}{1 - \chi \hat{\mathbf{u}}_i \cdot \hat{\mathbf{u}}_j} \right\} \right]^{-1/2}, \tag{19}$$

although Eq. (15) is likely to be the more useful form in practice (when χ is imaginary, for example). We note that the great similarity between this generalized $\sigma(\hat{\mathbf{u}}_i, \hat{\mathbf{u}}_j, \hat{\mathbf{r}}_{ij})$ and that of Berne and Pechukas ensures that any computational overhead associated with its use will be trivial.

In Sec. IV we go on to discuss a full implementation of Eq. (15) in the Gay-Berne potential; here we comment briefly on certain limiting cases. Firstly, we note that on setting $l_i = l_j$ and $d_i = d_j$, we regain the identical particle result of Berne and Pechukas: the expression for χ reverts to that of Eq. (4), while σ_0 and α go to $\sqrt{2}d$ and unity, respectively.

If one of the particles is made spherical, for example, $l_i = d_i = d$, then both χ and α go to zero. The range parameter, nevertheless, remains finite in this limit and tends smoothly to

$$\sigma(\hat{\mathbf{u}}_j, \hat{\mathbf{r}}_{ij}) = \sigma_0 [1 - \chi \alpha^{-2} (\hat{\mathbf{r}}_{ij} \cdot \hat{\mathbf{u}}_j)^2]^{-1/2}, \tag{20}$$

where

$$\frac{\chi}{\alpha^2} = \frac{l_j^2 - d_j^2}{l_j^2 + d^2}. \tag{21}$$

We note that this is consistent with the rod-sphere form given in Ref. [9].

Finally, if we consider the case where one of the particles is oblate while the other is prolate, we note that both χ and α^2 become imaginary. This particular choice of parameters follows from the original derivation of Berne and Pechukas [9]. An alternative choice of parameters based on the (always real) coefficients $\alpha^{\pm 2}\chi$ and χ^2 employed in Eq. (15) can be postulated simply. Such a choice is made in Sec. III B. Thus, the range parameter we have derived can be used for all choices of l's and d's, and is fully consistent with the equivalent functions suggested previously for systems of identical particles and of rod-sphere mixtures.

B. Uniaxial and biaxial ellipsoids via the Perram-Wertheim route

The route just outlined does not represent the only approach by which to calculate the uniaxial range parameter. It has been shown by Perram *et al.* [15] that the range parameter of Berne and Pechukas' Gaussian overlap potential is identical to a simple approximation of the hard-ellipsoid contact function due to Perram and Wertheim [16]. The true overlap function for hard ellipsoids i, j may be written in the form

$$F^{\mathrm{PW}}(\hat{\mathbf{u}}_i, \hat{\mathbf{u}}_j, \mathbf{r}_{ij}) = r_{ij}^2 f^{\mathrm{PW}}(\hat{\mathbf{u}}_i, \hat{\mathbf{u}}_j, \hat{\mathbf{r}}_{ij}) = r_{ij}^2 \max_{0 \leqslant \lambda \leqslant 1} f_\lambda(\hat{\mathbf{u}}_i, \hat{\mathbf{u}}_j, \hat{\mathbf{r}}_{ij}), \tag{22}$$

where $f^{\mathrm{PW}}(\hat{\mathbf{u}}_i, \hat{\mathbf{u}}_j, \hat{\mathbf{r}}_{ij})$ and $f_\lambda(\hat{\mathbf{u}}_i, \hat{\mathbf{u}}_j, \hat{\mathbf{r}}_{ij})$ depend on particle *orientations*, not separations, and $f_\lambda(\hat{\mathbf{u}}_i, \hat{\mathbf{u}}_j, \hat{\mathbf{r}}_{ij})$ additionally has a parametric dependence on λ. All of these functions also depend on the dimensions of the ellipsoids. When $F^{\mathrm{PW}}(\hat{\mathbf{u}}_i, \hat{\mathbf{u}}_j, \mathbf{r}_{ij}) < 1$ the two ellipsoids overlap; when $F^{\mathrm{PW}}(\hat{\mathbf{u}}_i, \hat{\mathbf{u}}_j, \mathbf{r}_{ij}) > 1$ they do not; $F^{\mathrm{PW}}(\hat{\mathbf{u}}_i, \hat{\mathbf{u}}_j, \mathbf{r}_{ij}) = 1$ is the tangency condition. Explicit expressions for $F^{\mathrm{PW}}(\hat{\mathbf{u}}_i, \hat{\mathbf{u}}_j, \mathbf{r}_{ij})$ are given by Perram and Wertheim [16] for the case of general spheroids (not necessarily identical) and for the special case of identical, axially symmetric, ellipsoids of revolution. The expression is equivalent to Vieillard-Baron's criterion [19] for ellipsoid overlap; some discussion of the two approaches, and their use in simulations, appears elsewhere [2]. Because of the scaling with r_{ij}^2 evident in the above equation, it is clear that

$$\sigma^{\mathrm{PW}}(\hat{\mathbf{u}}_i, \hat{\mathbf{u}}_j, \hat{\mathbf{r}}_{ij}) \equiv \frac{1}{\sqrt{f^{\mathrm{PW}}(\hat{\mathbf{u}}_i, \hat{\mathbf{u}}_j, \hat{\mathbf{r}}_{ij})}} \tag{23}$$

is the distance of closest approach for hard ellipsoids with the specified orientations.

As pointed out in [15], and echoed in [2], $\sigma^{\mathrm{PW}}(\hat{\mathbf{u}}_i, \hat{\mathbf{u}}_j, \hat{\mathbf{r}}_{ij})$ reduces to the Gaussian overlap range parameter if λ is set to $\frac{1}{2}$, i.e.,

$$\sigma(\hat{\mathbf{u}}_i, \hat{\mathbf{u}}_j, \hat{\mathbf{r}}_{ij}) \equiv \frac{1}{\sqrt{f_{1/2}(\hat{\mathbf{u}}_i, \hat{\mathbf{u}}_j, \hat{\mathbf{r}}_{ij})}}. \tag{24}$$

Since $f_\lambda(\hat{\mathbf{u}}_i, \hat{\mathbf{u}}_j, \hat{\mathbf{r}}_{ij})$ for $\lambda \neq \lambda_{\max}$ is an underestimate of $f^{\mathrm{PW}}(\hat{\mathbf{u}}_i, \hat{\mathbf{u}}_j, \hat{\mathbf{r}}_{ij})$, so $\sigma(\hat{\mathbf{u}}_i, \hat{\mathbf{u}}_j, \hat{\mathbf{r}}_{ij})$ is an *overestimate* of the distance of closest approach for two hard ellipsoids [2,15]. Thus, in some sense, Berne and Pechukas' Gaussian overlap shape parameter can be viewed as a simplified approximation to the hard-ellipsoid contact function.

For the case of nonequivalent uniaxial ellipsoids, we can easily verify that $f_{1/2}(\hat{\mathbf{u}}_i,\hat{\mathbf{u}}_j,\hat{\mathbf{r}}_{ij})$ is indeed equal to $\sigma(\hat{\mathbf{u}}_i,\hat{\mathbf{u}}_j,\hat{\mathbf{r}}_{ij})$ as defined in Eq. (15). From Ref. [16], for two axially symmetric ellipsoids with principal semiaxes of length a_i,a_j, and degenerate transverse semiaxes of length b_i,b_j, we obtain

$$f_{1/2}(\hat{\mathbf{u}}_i,\hat{\mathbf{u}}_j,\hat{\mathbf{r}}_{ij})=\frac{1}{4\Delta}\left[1+\frac{c_x(\hat{\mathbf{r}}_{ij}\cdot\hat{\mathbf{u}}_i)^2+c_y(\hat{\mathbf{r}}_{ij}\cdot\hat{\mathbf{u}}_j)^2+c_xc_y(\hat{\mathbf{r}}_{ij}\cdot\hat{\mathbf{u}}_i)(\hat{\mathbf{r}}_{ij}\cdot\hat{\mathbf{u}}_j)(\hat{\mathbf{u}}_i\cdot\hat{\mathbf{u}}_j)}{1-c_xc_y(\hat{\mathbf{u}}_i\cdot\hat{\mathbf{u}}_j)^2}\right], \tag{25}$$

where

$$\begin{aligned}\Delta&=\tfrac{1}{2}(b_i^2+b_j^2),\\ c_x&=\frac{b_i^2-a_i^2}{b_j^2+a_i^2},\\ c_y&=\frac{b_j^2-a_j^2}{b_i^2+a_j^2}.\end{aligned} \tag{26}$$

Some elementary manipulations are sufficient to show that this is identical to Eq. (15), with

$$\begin{aligned}\chi^2&=c_xc_y,\\ \chi\alpha^2&=-c_x,\\ \chi/\alpha^2&=-c_y,\\ \sigma_0^2&=4\Delta.\end{aligned} \tag{27}$$

Unlike χ and α^2, the parameters c_x, c_y, and Δ are always real. Note also that the original Gaussian overlap ''length'' and ''breadth'' parameters map onto the semiaxis lengths as $l_i=\sqrt{2}a_i$ and $d_i=\sqrt{2}b_i$. Thus, for two identical spheres, $\sigma_0=2b=\sqrt{2}d$. Note also the nonadditivity of the radii for unequal spheres, a consequence of the approximation made in setting $\lambda=1/2$.

For the biaxial form of the Gay-Berne potential, there is, again, a direct, approximate, relationship between the Gaussian overlap $\sigma(\hat{\mathbf{u}}_i,\hat{\mathbf{u}}_j,\hat{\mathbf{r}}_{ij})$ and an underlying hard-spheroid overlap function. Once more we follow the derivation of Perram and co-workers [15,16]; see also Ref. [2], Eqs. (2.85)–(2.96). It is useful to define the three orthogonal semiaxis vectors for each molecule i,

$$\mathbf{a}_i^\beta=a_i^\beta\hat{\mathbf{u}}_i^\beta;\quad \beta=x,y,z, \tag{28}$$

where $\hat{\mathbf{u}}_i^\beta$ are the corresponding unit vectors and a_i^β the semiaxis lengths. Then a dyadic matrix is defined for each molecule:

$$\underline{\mathbf{A}}_i\equiv\sum_\beta \mathbf{a}_i^\beta\otimes\mathbf{a}_i^\beta=\sum_\beta (a_i^\beta)^2\hat{\mathbf{u}}_i^\beta\otimes\hat{\mathbf{u}}_i^\beta. \tag{29}$$

The form for the reduced Perram-Wertheim function is

$$f_\lambda(\{\hat{\mathbf{u}}_i^\beta\},\{\hat{\mathbf{u}}_j^\beta\},\hat{\mathbf{r}}_{ij})=\lambda(1-\lambda)\hat{\mathbf{r}}_{ij}\cdot\underline{\mathbf{G}}\cdot\hat{\mathbf{r}}_{ij}, \tag{30}$$

where

$$\underline{\mathbf{G}}=[(1-\lambda)\underline{\mathbf{A}}_i+\lambda\underline{\mathbf{A}}_j]^{-1}. \tag{31}$$

In computer simulations, it is straightforward to perform the 3×3 matrix inversion on the right-hand side of Eq. (31) numerically, and thus determine the shape parameter. This is the procedure adopted by Allen [20] for $f_\lambda(\{\hat{\mathbf{u}}_i^\beta\},\{\hat{\mathbf{u}}_j^\beta\},\hat{\mathbf{r}}_{ij})$ in simulating biaxial hard spheroids using the exact Perram-Wertheim criterion. A faster alternative, remarked in Ref. [15] is to calculate Eq. (30) as the scalar product $\mathbf{r}\cdot\mathbf{X}$ where $\mathbf{X}$ is the solution of the linear equations $\underline{\mathbf{C}}X=\mathbf{r}$.

However, it is also possible to express the inverse analytically. For the case $\lambda=\frac{1}{2}$, we may write [see Eqs. (2.95)–(2.96) of Ref. [2]]

$$\underline{\mathbf{G}}=2\left[\frac{(\underline{\mathbf{A}}_i+\underline{\mathbf{A}}_j)^2-c_1(\underline{\mathbf{A}}_i+\underline{\mathbf{A}}_j)+c_2\underline{\mathbf{I}}}{c_3}\right], \tag{32}$$

where

$$c_1=\sum_\beta [(a_i^\beta)^2+(a_j^\beta)^2], \tag{33a}$$

$$c_2=(a_i^x)^2(a_i^y)^2+(a_i^y)^2(a_i^z)^2+(a_i^z)^2(a_i^x)^2+(a_j^x)^2(a_j^y)^2+(a_j^y)^2(a_j^z)^2+(a_j^z)^2(a_j^x)^2+\left[\sum_\beta (a_i^\beta)^2\right]\left[\sum_\beta (a_j^\beta)^2\right]-\sum_\beta (\mathbf{a}_i^\beta\cdot\mathbf{a}_j^\beta)^2, \tag{33b}$$

$$c_3=(a_i^x)^2(a_i^y)^2(a_i^z)^2+(a_j^x)^2(a_j^y)^2(a_j^z)^2+\sum_{\beta\delta\kappa}\left[\frac{1}{2}(\mathbf{a}_i^\beta\times\mathbf{a}_i^\delta\cdot\mathbf{a}_j^\kappa)^2+\frac{1}{2}(\mathbf{a}_j^\beta\times\mathbf{a}_j^\delta\cdot\mathbf{a}_i^\kappa)^2\right]. \tag{33c}$$

The contractions with $\hat{\mathbf{r}}_{ij}$ that lead from $\underline{\mathbf{G}}$ to $f_{1/2}(\{\hat{\mathbf{u}}_i^\beta\},\{\hat{\mathbf{u}}_j^\beta\},\hat{\mathbf{r}}_{ij})$ are easily done, with

$$\hat{\mathbf{r}}_{ij}\cdot\underline{\mathbf{A}}_i\cdot\hat{\mathbf{r}}_{ij}=\sum_\beta (\mathbf{a}_i^\beta\cdot\hat{\mathbf{r}}_{ij})^2,\quad \hat{\mathbf{r}}_{ij}\cdot\underline{\mathbf{A}}_i^2\cdot\hat{\mathbf{r}}_{ij}=\sum_\beta (a_i^\beta)^2(\mathbf{a}_i^\beta\cdot\hat{\mathbf{r}}_{ij})^2,\quad \hat{\mathbf{r}}_{ij}\cdot\underline{\mathbf{A}_i\mathbf{A}_j}\cdot\hat{\mathbf{r}}_{ij}=\sum_{\beta\delta}(\mathbf{a}_i^\beta\cdot\mathbf{a}_j^\delta)(\mathbf{a}_i^\beta\cdot\hat{\mathbf{r}}_{ij})(\mathbf{a}_j^\delta\cdot\hat{\mathbf{r}}_{ij}). \tag{34}$$

The final result is

$$f_{1/2}(\{\hat{\mathbf{u}}_i^\beta\},\{\hat{\mathbf{u}}_j^\beta\},\hat{\mathbf{r}}_{ij})=\frac{1}{2c_3}\left\{\sum_\beta\left[(a_i^\beta)^2(\mathbf{a}_i^\beta\cdot\hat{\mathbf{r}}_{ij})^2+(a_j^\beta)^2(\mathbf{a}_j^\beta\cdot\hat{\mathbf{r}}_{ij})^2\right]+2\sum_{\beta\delta}(\mathbf{a}_i^\beta\cdot\mathbf{a}_j^\delta)(\mathbf{a}_i^\beta\cdot\hat{\mathbf{r}}_{ij})(\mathbf{a}_j^\delta\cdot\hat{\mathbf{r}}_{ij})\right.$$
$$\left.-c_1\sum_\beta\left[(\mathbf{a}_i^\beta\cdot\hat{\mathbf{r}}_{ij})^2+(\mathbf{a}_j^\beta\cdot\hat{\mathbf{r}}_{ij})^2\right]+c_2\right\}. \tag{35}$$

The Gaussian overlap shape parameter may again be written $\sigma(\hat{\mathbf{u}}_i,\hat{\mathbf{u}}_j,\hat{\mathbf{r}}_{ij})=1/\sqrt{f_{1/2}(\hat{\mathbf{u}}_i,\hat{\mathbf{u}}_j,\hat{\mathbf{r}}_{ij})}$, and is again, rigorously, an overestimate of the true closest approach distance of hard spheroids at the specified orientations. Comparing Eqs. (35) and (15), we can see that the two are of the same basic form: both give a $\sigma(\hat{\mathbf{u}}_i,\hat{\mathbf{u}}_j,\hat{\mathbf{r}}_{ij})$ with a numerator determined by scalar (triple) products of semiaxis vectors, and a denominator involving scalar products of axis vectors with the center-center direction vector $\hat{\mathbf{r}}_{ij}$. Equation (35) becomes identical to (15) in the limit that both of the particles involved are made uniaxial.

C. Other approaches

Before closing this section, we note that we have found another route to Eqs. (15)–(19) based simply on the behavior of the shape parameter in the five configurations shown in Table I. Following the original result of Berne and Pechukas, we assumed the shape parameter to be given by a minimally modified form of Eq. (3) and took $\sigma(\hat{\mathbf{u}}_i,\hat{\mathbf{u}}_j,\hat{\mathbf{r}}_{ij})$ to be given by the root mean square of the appropriate pair of l_i, l_j, d_i, and d_j for each of the five configurations [e.g., for the side-side arrangement, taking $\sigma^2=0.5(d_i^2+d_j^2)$]. While this approach is clearly unsatisfactory in isolation, its success in yielding the correct final expressions demonstrates that the behavior of the Gaussian overlap range parameter is both simple and intuitive.

While the Perram-Wertheim approach offers the simplest route to $\sigma(\hat{\mathbf{u}}_i,\hat{\mathbf{u}}_j,\hat{\mathbf{r}}_{ij})$ for the generalized particle shapes we are concerned with here, it lacks clear physical interpretation. The impact of setting $\lambda=\frac{1}{2}$ is far from obvious, and an interaction potential based on this approximation is hard to justify until reference is made to the origins of the Gaussian overlap approach.

The ellipsoid contact function itself, $f_\lambda(\hat{\mathbf{u}}_i,\hat{\mathbf{u}}_j,\hat{\mathbf{r}}_{ij})$ at $\lambda=\lambda_{\max}$, has some advantages over $\sigma(\hat{\mathbf{u}}_i,\hat{\mathbf{u}}_j,\hat{\mathbf{r}}_{ij})$, such as its adherence to the Lorentz-Berthelot additivity rule. However, the crucial point in favor of the latter is its simple analytical form, which is easily differentiable. It can, therefore, be used in molecular dynamics simulations using ''soft'' interaction potentials (this is not practicable with the ellipsoid contact function, which would require numerical differentiation to calculate each force contribution). Thus, while it may be of interest to perform a Monte Carlo simulation employing the ellipsoid contact function, $\sigma(\hat{\mathbf{u}}_i,\hat{\mathbf{u}}_j,\hat{\mathbf{r}}_{ij})$ remains a significant and more convenient alternative.

IV. APPLICATION TO THE GAY-BERNE MODEL

A. The Gay-Berne strength parameter

The task of importing the generalized shape parameter into the Gay-Berne potential involves little more than inserting Eqs. (15)–(18) into Eq. (7). However, the strength anisotropy term of Eq. (9) also needs to be modified; if it were not, then the well depths for the two different T configurations (see Table I) would be equal. By reference to our shape parameter result we suggest use of the form

$$\varepsilon_2(\hat{\mathbf{u}}_i,\hat{\mathbf{u}}_j,\hat{\mathbf{r}}_{ij})=1-\chi'\left\{\frac{\alpha'^2(\hat{\mathbf{r}}_{ij}\cdot\hat{\mathbf{u}}_i)^2+\alpha'^{-2}(\hat{\mathbf{r}}_{ij}\cdot\hat{\mathbf{u}}_j)^2-2\chi'(\hat{\mathbf{r}}_{ij}\cdot\hat{\mathbf{u}}_i)(\hat{\mathbf{r}}_{ij}\cdot\hat{\mathbf{u}}_j)(\hat{\mathbf{u}}_i\cdot\hat{\mathbf{u}}_j)}{1-\chi'^2(\hat{\mathbf{u}}_i\cdot\hat{\mathbf{u}}_j)^2}\right\}, \tag{36}$$

where, as previously, we have introduced a single new parameter, α'. The task of relating the parameters ε_0, μ, ν, χ', and α' to the system of interest is rather less clearcut than that experienced in deriving the shape parameter. As evidence of this, we note that there are currently a number of different strength anisotropy parametrizations being used for Gay-Berne systems with identical shape anisotropies [10,21].

In order to gain an indication of how these parameters relate to given configurations, we list, in Table I, the form of $\varepsilon(\hat{\mathbf{u}}_i,\hat{\mathbf{u}}_j,\hat{\mathbf{r}}_{ij})$ for each of the arrangements listed. From this we see that ε_0 is the only relevant parameter for the cross (X) arrangement and that ν controls the well-depth variation from the cross to the side-side (S) arrangement.

An initial route to determining the other three parameters is offered by noting that the expressions given in Table I represent a series of simultaneous equations in μ, χ', and α': a numerical solution of these equations should give a suitable starting point for a fit to a full potential. We stress that this does not represent a rigorous means by which to parametrize a given system, however, and urge that this matter be considered anew for each new set of l's and d's used.

Before attempting such a parametrization, we note that in the limit of identical particles, the two T configurations become equivalent, and α' goes to unity; Eq. (36) then reduces to the standard Gay-Berne relationship. Alternatively, if one of the particles is spherical, then the S, X, and, say, $T1$

arrangements, and the E and $T2$ arrangements become equivalent. As in the case of the range parameter, both χ' and α' then go to zero, while the product, $\chi'\alpha'^{-2}$, remains finite. Thus, the well-depth anisotropy function becomes

$$\varepsilon(\hat{\mathbf{u}}_j,\hat{\mathbf{r}}_{ij})=\varepsilon_0[1-\chi'\alpha'^{-2}(\hat{\mathbf{r}}_{ij}\cdot\hat{\mathbf{u}}_j)^2]^{\mu}, \tag{37}$$

where

$$\chi'\alpha'^{-2}=1-\left(\frac{\varepsilon_E}{\varepsilon_S}\right)^{1/\mu} \tag{38}$$

and $\varepsilon_S=\varepsilon_0$. For the rod-sphere interaction, the equivalence of the S and X arrangements requires that ν be zero. The remaining parameters, μ and $\chi'\alpha'^{-2}$ (if they are both to be used), can be obtained from a fit to the full potential.

B. Parametrization of a rod-disk interaction

In seeking a set of parameters suitable for modeling the interaction between a rodlike particle and a disklike particle, we have closely followed the procedure used by Luckhurst and co-workers in their analyses of the rod-rod and disk-disk parametrizations of the standard Gay-Berne model [11,17]. This is based on a Boltzmann weighted average of the interaction between a pair of molecules, calculated purely from the sum of atom-centered Lennard-Jones interactions. While this procedure has been found to yield potentials that overestimate the relative well-depth ratios of the various configurations (due to its neglect of molecular flexibility and other important factors such as quadrupolar interactions), it does offer an objective means by which to compare interactions between molecules of various shapes.

We have considered the interaction between the rodlike molecule *p*-terphenyl (the same basis molecule as was used in Ref. [17]) and the disklike molecule triphenylene (as used in Ref. [11]). In the following, we take $\hat{\mathbf{u}}_j$ to coincide with the para-axis of the *p*-terphenyl molecule and $\hat{\mathbf{u}}_i$ to run through the center of, and orthogonal to, the central ring of the triphenylene molecule. We have obtained an energy-minimized structure for each of these molecules using the computational chemistry package CERIUS^2 [22]. For this and for all subsequent calculations, we have used the same Lennard-Jones parameters as Luckhurst and Simmonds (explicitly, $\sigma_{CC}=3.35$ Å, $\varepsilon_{CC}/k_B=51.2$ K, $\sigma_{HH}=2.81$ Å, $\varepsilon_{HH}/k_B=8.6$ K as given in Allen and Tildesley [23]) and employed the Lorentz-Berthelot mixing rules. Keeping all internal degrees of freedom fixed, we have then calculated the interaction energy of the two molecules, $U(\hat{\mathbf{u}}_i,\hat{\mathbf{u}}_j,\mathbf{r}_{ij},\phi_i,\phi_j)$, where ϕ_i (ϕ_j) is the azimuthal angle of molecule i (j). This interaction energy is given by the sum of the Lennard-Jones contributions from all distinct pairs of atomic sites on different molecules. Thus,

$$U(\hat{\mathbf{u}}_i,\hat{\mathbf{u}}_j,\mathbf{r}_{ij},\phi_i,\phi_j)=\sum_{m=1}^{N_i}\sum_{n=1}^{N_j}4\varepsilon_{mn}\left[\left(\frac{\sigma_{mn}}{r_{mn}}\right)^{12}-\left(\frac{\sigma_{mn}}{r_{mn}}\right)^{6}\right], \tag{39}$$

where N_i (N_j) is the number of sites on molecule i (j). In order to obtain a full potential consistent with the cylindrical symmetry of our model particles, we have performed a Boltzmann-weighted average over the azimuthal variables for each chosen set of $\hat{\mathbf{u}}_i$, $\hat{\mathbf{u}}_j$, and $\mathbf{r}_{ij}$. In practice, this has been achieved by calculating the function

$$U_{\mathrm{av}}(\hat{\mathbf{u}}_i,\hat{\mathbf{u}}_j,\mathbf{r}_{ij})=\frac{\Sigma_{\phi_i}\Sigma_{\phi_j}U(\hat{\mathbf{u}}_i,\hat{\mathbf{u}}_j,\mathbf{r}_{ij},\phi_i,\phi_j)\exp[-U(\hat{\mathbf{u}}_i,\hat{\mathbf{u}}_j,\mathbf{r}_{ij},\phi_i,\phi_j)/k_BT]}{\Sigma_{\phi_i}\Sigma_{\phi_j}\exp[-U(\hat{\mathbf{u}}_i,\hat{\mathbf{u}}_j,\mathbf{r}_{ij},\phi_i,\phi_j)/k_BT]}. \tag{40}$$

To enable direct comparison of results, we have followed Luckhurst and Simmonds [17] in using a value of 500 K for T.

We have calculated $U_{\mathrm{av}}(\hat{\mathbf{u}}_i,\hat{\mathbf{u}}_j,\mathbf{r}_{ij})$ for a range of r_{ij} for each of the $\hat{\mathbf{u}}_i,\hat{\mathbf{u}}_j,\hat{\mathbf{r}}_{ij}$ combinations shown in Table I. The results of these calculations, which were obtained using a 1 degree increment in the azimuthal sums of Eq. (40), are shown as full lines in Fig. 1. We have performed a least-squares fit of our model potential to these data using the NAG minimization routine E04JAF. This fit is shown as the dashed lines in Fig. 1, and corresponds to the parameter values $\sigma_0=7.6$ Å; $\varepsilon_0/k_B=1380$ K; $\alpha^2\chi=-3.0$; $\chi^2=-5.7$; $\mu=3.8$; $\nu=0.13$; $\chi'\alpha'^2=-0.11$; $\chi'^2=0.46$.

From Fig. 1, we observe that this fit is quantitatively reasonable throughout. The properties that relate to the range parameter variables (i.e., the separations at which the potential first becomes attractive) are matched particularly well. All of the fitted curves have shallower minima than the corresponding $U_{\mathrm{av}}(\hat{\mathbf{u}}_i,\hat{\mathbf{u}}_j,\mathbf{r}_{ij})$ curves, indicating that the shifted 12-6 form of the Gay-Berne potential is generally unable to reproduce the shape of a potential composed of a sum of Lennard-Jones sites. A related discrepancy is that some of the long-ranged tails appear rather too attractive. Despite this, the relative well depths of four of the five $U_{\mathrm{av}}(\hat{\mathbf{u}}_i,\hat{\mathbf{u}}_j,\mathbf{r}_{ij})$ curves are well reproduced (the exception is the E curve, which is too shallow).

In their parametrization of the rod-rod potential, Luckhurst and Simmonds obtained a well-depth ratio $\varepsilon_S/\varepsilon_E$ of 39.6, with $\varepsilon_0/k_B=4302$ K [17]. Emerson, Luckhurst, and Whatling obtained $\varepsilon_E/\varepsilon_S=9$ for a disk-disk interaction [11] but did not report any absolute values. The greatest well-depth ratio we have found in our $U_{\mathrm{av}}(\hat{\mathbf{u}}_i,\hat{\mathbf{u}}_j,\mathbf{r}_{ij})$ data is 10.4 (11.4 in our fitted data), substantially less than the 39.6 found for the two rods. This, along with the respective ε_0 values obtained, supports intuitive arguments that in a mixture of (similarly sized) rods and disks, the strongest rod-disk interaction will be weaker than the strongest rod-rod and disk-disk interactions.

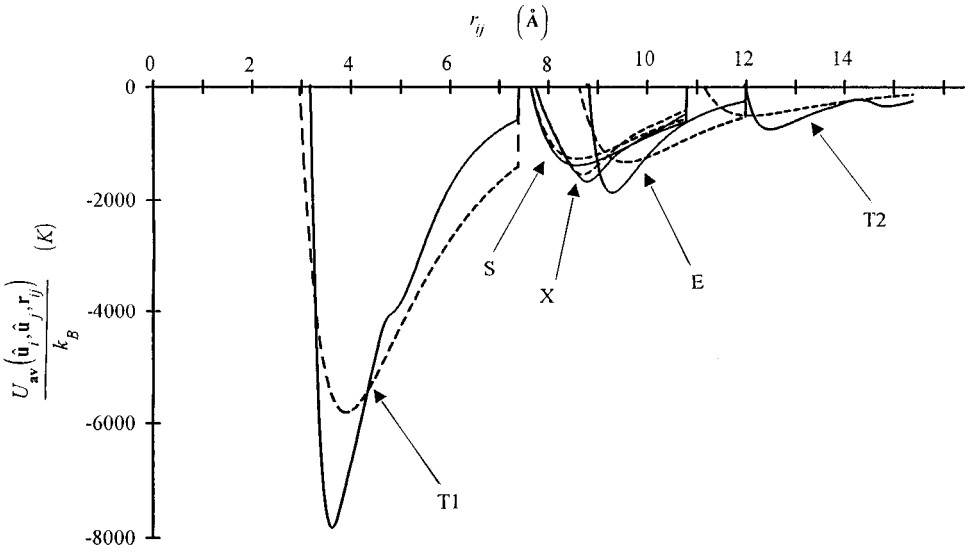

FIG. 1. $U_{\mathrm{av}}(\hat{\mathbf{u}}_i,\hat{\mathbf{u}}_j,\mathbf{r}_{ij})$ data (solid lines) for the azimuthally averaged interaction potential of *p*-terphenyl and triphenylene, and associated fit of the generalized Gay-Berne model (dashed lines). See text for fit parameters. The fits were generated using data from a limited range of r_{ij} values; the upper limit of this range, for each of the curves shown, is indicated by the vertical discontinuity at large r_{ij}.

The value we have obtained for the exponent μ is broadly similar to that used in the various simulations of identical Gay-Berne particles [10,11,17,21]. Our value for ν is substantially smaller than that used for such systems, however. Such a difference is to be expected; the relevant part of the strength anisotropy function, $\varepsilon_1(\hat{\mathbf{u}}_i,\hat{\mathbf{u}}_j)$, is itself much bigger than that used in the identical particle interaction, due to the negative value of χ^2 [recall Eqs. (6) and (8)]. Small ν values should, therefore, be a feature of all rod-disk parametrizations.

The remaining parameters of our fit do not naturally lend themselves to specific discussion. We note that the (unprimed) shape parameter variables obtained have given very good agreement with the input data for the specific case considered here. This supports continued use of potentials based on the Gaussian overlap shape parameter. The main failure of the fit is that it underestimates the relative depth of the *E* arrangement. This, along with the general shallowness of the fitted curves, may indicate that an alternative to the shifted 12-6 Gay-Berne potential form may yield closer agreement to realistic molecule-molecule interactions. This must remain a rather tentative conclusion, however, given the relatively crude molecular model compared with in this work.

In conclusion, we have developed a generalized version of the Gay-Berne potential, which enables calculation of the interaction between dissimilar uniaxial or biaxial particles. This interaction potential reduces to the standard Gay-Berne and Lennard-Jones forms in the appropriate limits. As such, it is appropriate for use in a number of simulation systems involving mixtures or assemblies of non-spherical interaction sites.

ACKNOWLEDGMENTS

This work arose from discussions held at the meetings of the CCP5-sponsored complex fluid simulators consortium and the British Liquid Crystal Society in March 1994. The authors acknowledge useful conversations with many members of the former, particularly M. R. Wilson and A. P. J. Emerson. We also thank J. W. Perram for providing Ref. [15] and C. Zannoni for communicating details of work in progress (Ref. [12]).

[1] For reviews of this subject see D. Frenkel, Mol. Phys. **60**, 1 (1987); M. P. Allen, Philos. Trans. R. Soc. London A **344**, 323 (1993).

[2] M. P. Allen, G. T. Evans, D. Frenkel, and B. M. Mulder, Adv. Chem. Phys. **86**, 1 (1993).

[3] M. P. Allen and M. R. Wilson, J. Comput. Aided Mol. Des. **3**, 335 (1989); M. P. Allen, in Observation, *Prediction and Simulation of Phase Transitions in Complex Fluids*, Proceedings of International School of Physics ''Enrico Fermi,'' Course CXXIX, Varenna, 1994, edited by M. Baus, L. Rull, and J.-P. Ryckaert (Kluwer, Dordrecht, 1995).

[4] G. R. Luckhurst and S. Romano, Proc. R. Soc. London A **373**, 111 (1980).

[5] M. D. De Luca, M. P. Neal, and C. M. Care, Liq. Cryst. **16**, 257 (1994); M. P. Neal, M. D. De Luca, and C. M. Care, Mol. Sim. **14**, 245 (1995).

[6] G. V. Paoloni, G. Ciccotti, and M. Ferrario, Mol. Phys. **80**, 297 (1993).

[7] S. J. Picken, W. F. van Gunsteren, P. Th. van Duijnen, and W. H. de Jeu, Liq. Cryst. **6**, 357 (1989); M. R. Wilson and M. P. Allen, Mol. Cryst. Liq. Cryst. **198**, 465 (1991); M. R. Wilson and M. P. Allen, Liq. Cryst. **12**, 157 (1992).

[8] J. G. Gay and B. J. Berne, J. Chem. Phys. **74**, 3316 (1981).

[9] B. J. Berne and P. Pechukas, J. Chem. Phys. **64**, 4213 (1972).

[10] D. J. Adams, G. R. Luckhurst, and R. W. Phippen, Mol. Phys. **61**, 1575 (1987); G. R. Luckhurst, R. W. Phippen, and R. A. Stephens, Liq. Cryst. **8**, 451 (1990); E. De Miguel, L. F. Rull, M. K. Chalam, and K. E. Gubbins, Mol. Phys. **74**, 405 (1991); S. Sarman and D. J. Evans, J. Chem. Phys. **99**, 9021 (1993); R. Berardi, A. P. J. Emerson, and C. Zannoni, J. Chem. Soc. Faraday Trans. **89**, 4069 (1993).

[11] A. P. J. Emerson, G. R. Luckhurst, and S. G. Whatling, Mol. Phys. **82**, 113 (1994).
[12] R. Berardi, C. Fava, and C. Zannoni, Chem. Phys. Lett. **236**, 462 (1995).
[13] P. S. J. Simmonds, Ph.D. thesis, University of Southampton, 1990 (unpublished).
[14] A. P. J. Emerson and G. R. Luckhurst (private communication); M. P. Neal, A. J. Parker, and C. M. Care (unpublished).
[15] J. W. Perram, E. Praestgaard, J. Rasmussen, and J. Lebowitz (unpublished).
[16] J. W. Perram and M. S. Wertheim, J. Comput. Phys. **58**, 409 (1985).
[17] G. R. Luckhurst and P. S. J. Simmonds, Mol. Phys. **80**, 233 (1993).
[18] J. Kushick and B. J. Berne, J. Chem. Phys. **64**, 1362 (1976).
[19] J. Vieillard-Baron, J. Chem. Phys. **56**, 4729 (1972).
[20] M. P. Allen, Liq. Cryst. **8**, 499 (1990).
[21] R. Berardi, A. P. J. Emerson, and C. Zannoni, J. Chem. Soc. Faraday Trans. **89**, 4069 (1993).
[22] Energy minimized single-molecule structures were generated using the program CERIUS^2 ™. This program was developed by Molecular Simulations Incorporated. Subsequent generation of $U_{\rm av}(\hat{\mathbf{u}}_i,\hat{\mathbf{u}}_j,\mathbf{r}_{ij})$ data was performed using in-house codes.
[23] M. P. Allen and D. J. Tildesley, *Computer Simulation of Liquids* (Clarendon, Oxford, 1989).